Supporting Information for 'Monitoring Isomerization of Molecules in Solution using Ion Mobility Mass Spectrometry'

James N. Bull,[†] Michael S. Scholz,[†] Neville J. A. Coughlan,[†] Akio Kawai,[‡] and Evan J. Bieske[*,†]

[†]School of Chemistry, University of Melbourne, Melbourne VIC 3010, Australia

[‡]Department of Chemistry, Graduate School of Science and Engineering, Tokyo Institute of Technology, Ohokayama, Meguro-ku, Tokyo 152-8551, Japan

E-mail: evanjb@unimelb.edu.au

LED array

Photographs of the LED array used to irradiate the syringe and for capillary irradiation are shown in Figure S1. Each LED was driven at $2.8 - 3.3$ V and computer controlled with a Phidgets model $0/0/8$ relay board.
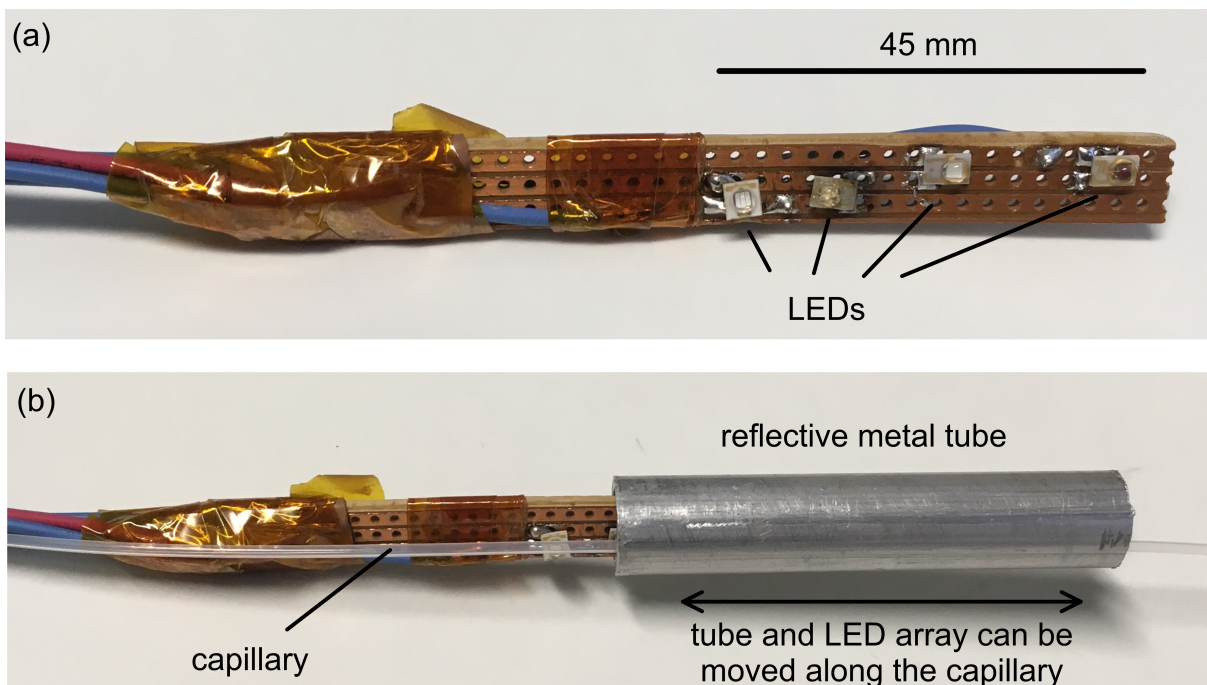

Figure S1: (a) Photograph of the unmounted LED array. (b) Photograph of the LED array, capillary, and reflective metal tube.

Density functional theory calculations of equilibrium geometries

Equilibrium geometries and relative energies of the target azoheteroarene isomers were calculated at the ωB97X-D$//$cc-pVTZ level of theory using Gaussian 09.[1–3] Equilibrium geometries were confirmed as structural minima through harmonic vibrational frequency analysis, which also provided zero-point energy corrections. Equilibrium geometries of E and Z-isomers are shown in Figure S2. In all cases, the E-isomer is predicted to be more stable in the gas phase than the Z-isomer.
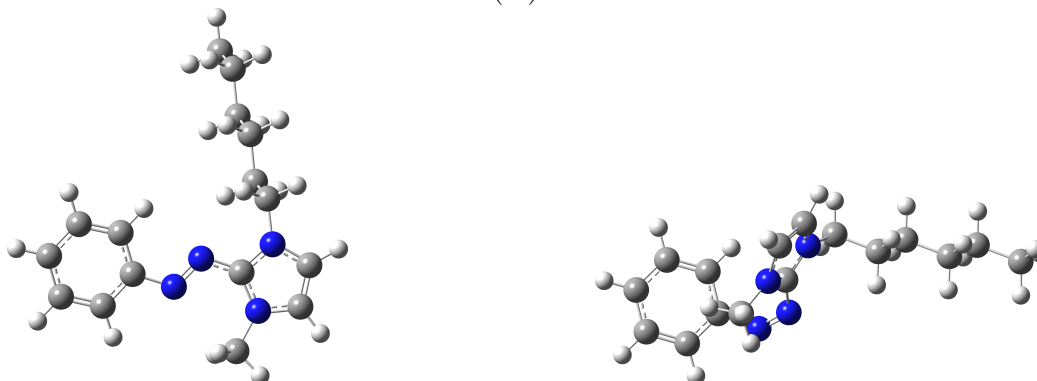
Mmim: $\Delta E(Z)=56\,\mathrm{kJ\,mol^{-1}}$
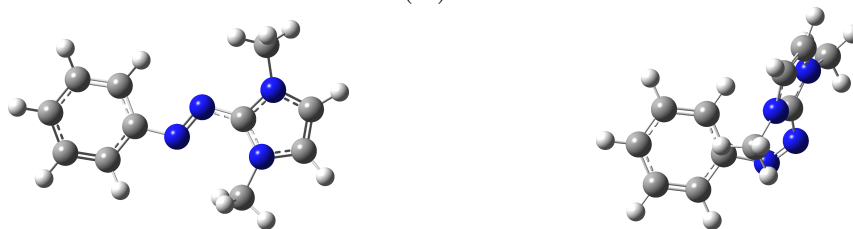
Bmim: $\Delta E(Z)=59\,\mathrm{kJ\,mol^{-1}}$
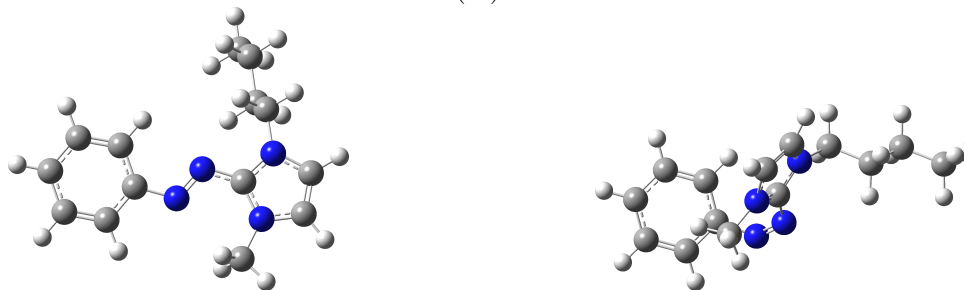
Hmim: $\Delta E(Z)=57\,\mathrm{kJ\,mol^{-1}}$

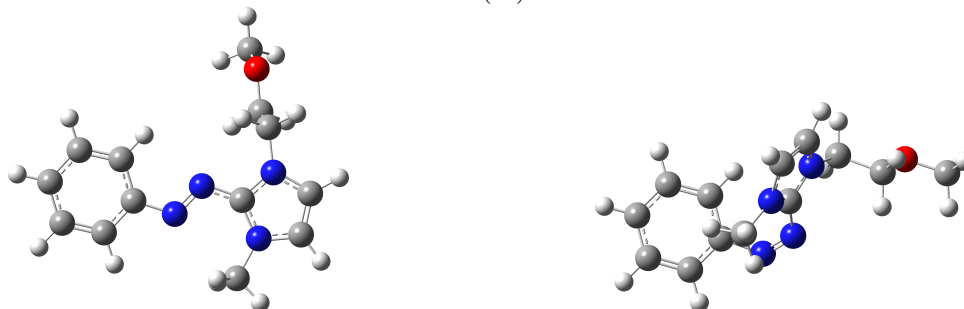MOEmim: $\Delta E(Z)=58\,\mathrm{kJ\,mol^{-1}}$

Figure S2: Equilibrium geometries for E (left) and Z (right) isomers for each of the four 2-phenylazo-methylimidazolium cations determined at the DFT ωB97X-D//cc-pVTZ level of theory. The energy of the Z-isomer relative to the E-isomer $[\Delta E(Z)]$ is given in each case. $\Delta E(Z)$ values are corrected for vibrational zero-point energy.

3

Collision cross-sections

Calculated Cross Sections

Isomer collision cross-sections, Ω_c, were calculated using MOBCAL with the trajectory method, with intermolecular interactions parametrised for N_2 and charge distributions obtained from the Merz-Singh-Kollman scheme constrained to reproduce the electric dipole moment.[4,5] Sufficient trajectories were computed for each isomer to give standard deviations of $\pm 1\,\text{Å}^2$. Calculated cross sections (Ω_c) are compiled in Table S1.

For the four 2-phenylazo-methylimidazolium cations, the more stable E-isomer is predicted to have a larger collision cross section than the Z-isomer supporting the assignment of the slow and fast ATD peaks to E and Z isomers, respectively. This assignment is consistent with the dominance of the slower peak (the more stable E-isomer) when the first ion funnel is driven at high RF potential, encouraging more violent collisions before injection into the drift region.

Measured Cross Sections

Measured collision cross sections were calibrated by recording arrival time distributions of the target ions along with tetraalkylammonium cations for which collision cross sections have been published.[4,7] An example ATD obtained from a mixture of [2PA-MOEmim]$^+$ and tetraalkylammonium salt cations is shown in Figure S3a.

The calibration procedure involved recognizing the relationship between an ion's transit

Table S1: Calculated and measured collision cross-sections (Ω_c and Ω_m, respectively, with Å^2 units) for the four 2-phenylazo-methylimidazolium cations in N_2. Relative errors for Ω_m values are estimated to be $\pm 0.5\,\text{Å}^2$. Percentage differences in the E and Z isomer cross sections are given in the last two columns.

	$\Omega_c(Z)$	$\Omega_m(Z)$	$\Omega_c(E)$	$\Omega_m(E)$	$\Delta\Omega_c$	$\Delta\Omega_m$
[2PA-Mmim]$^+$	143.5	138.3	146.3	141.6	2.0%	2.4%
[2PA-Bmim]$^+$	161.3	153.3	164.0	157.0	1.7%	2.4%
[2PA-Hmim]$^+$	176.9	165.6	180.1	167.9	1.8%	1.4%
[2PA-MOEmim]$^+$	159.7	149.9	161.3	155.2	1.0%	3.5%

time through the drift region (t_d), its mobility (K), and the temperature-dependent integral collision cross-section [Ω], through the Mason-Schamp equation,[6]

$$K = \frac{3ze}{16N} \sqrt{\frac{2\pi}{\mu k_B T}} \left(\frac{1}{\Omega}\right) = \frac{l^2}{t_d V}. \tag{1}$$

Here, z is the charge of the ion, e is the elementary charge, N is the number density of the buffer gas, μ is the reduced mass of the ion-neutral collision pair, k_B is the Boltzmann constant, T is the effective temperature, l is the length of the drift region, and V is the potential drop across the drift region.

In our instrument the measured arrival time of an ion packet, t, is given by:

$$t = t_d + t_{oct} + t_{quad} \tag{2}$$

where t_d, t_{oct}, and t_{quad} are the ion transit times through the drift region ($\approx$7 torr), octupole ion guide ($\approx$2$\times$10^{-4} torr), and quadrupole mass filter ($\approx$10^{-6} torr), respectively. Values of t_{oct} and t_{quad} were calculated from instrument parameters (dimensions and electrical potentials of the octupole ion guide and quadrupole mass filter) and are short ($\approx$0.1 ms) compared with t_d (7-18 ms). Equation 1 can be arranged to give a linear relation between collision cross section and $t_d\mu^{-1/2}$,

$$\Omega = At_d\mu^{-1/2} \tag{3}$$

where the constant A depends on pressure and temperature and is determined by plotting literature values of the collision cross sections (Ω_m) of the tetra-alkylammonium cations[4,7] against measured values of $t_d\mu^{-1/2}$ (see Figure S3b). Once A is determined, the cross sections (Ω_m) for the E and Z isomers of the 2-phenylazo-methylimidazolium cations can be ascertained. Resulting Ω_m values are compiled in Table S1. Calculated cross sections exceed measured values by $\approx$5% (Figure S3c), suggesting that theory systematically overestimates the actual cross sections.
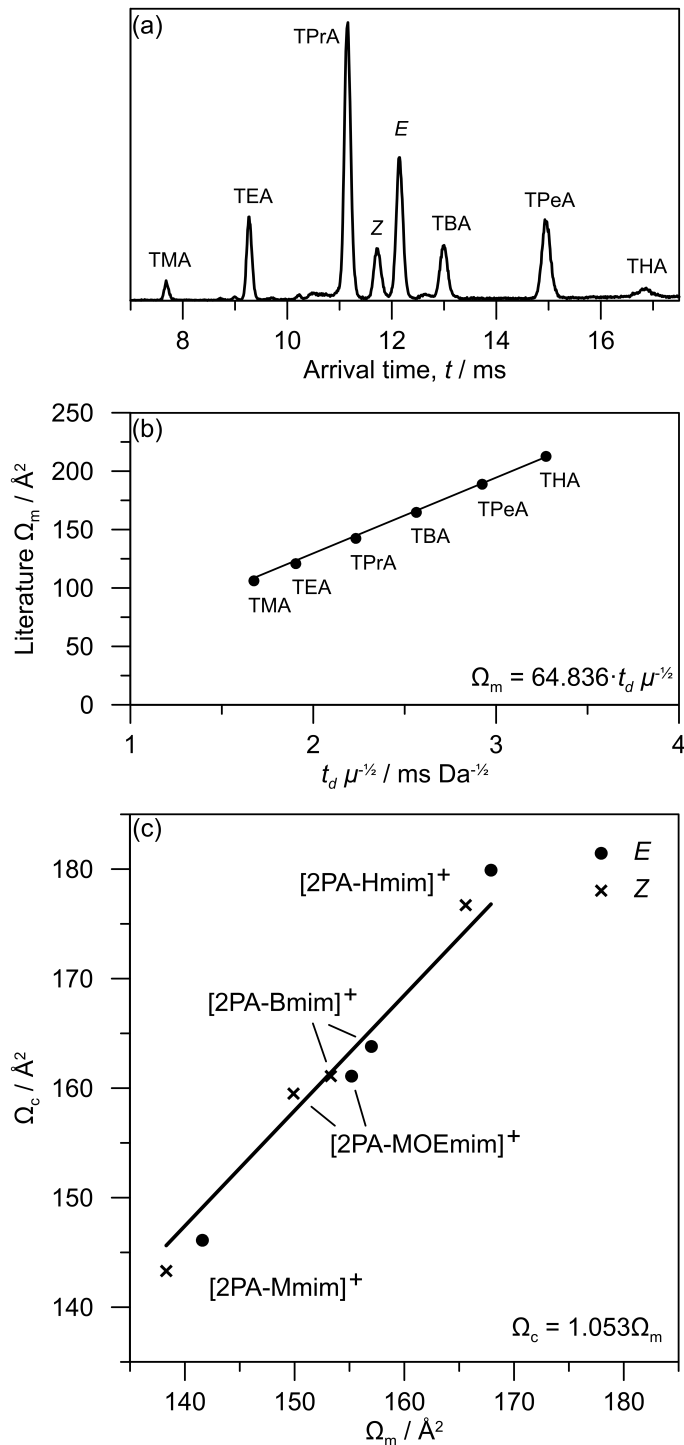
5

Figure S3: (a) Example ATD of [2PA-MOEmim]$^+$ and tetraalkylammonium salt mixture with 385 nm capillary irradiation and quadrupole mass selection turned off. Unassigned peaks are due to solvent adducts. (b) Correlation between $t_d\mu^{-1/2}$ and literature collision cross-sections, Ω_m for tetra-alkylammonium cations taken from refs. 4 and 7. (c) Ω_c plotted against Ω_m revealing a $\approx 5\%$ overestimation by theory. In (a) and (b), TMA= tetramethylammonium, TEA= tetraethylammonium, TPrA= tetrapropylammonium, TBA= tetrabutylammonium, TPeA= tetrapentylammonium, THA= tetrahexylammonium.

UV-Vis measurements for *Z-E* thermal isomerization rates

Z-E thermal isomerization for the azoheteroarenes was followed using a Varian Cary 50 Bio UV-Vis spectrophotometer by monitoring absorption of the solution in a quartz cuvette. The monitor wavelength was 385 nm, close to the absorption maximum of the *E*-isomer. Prior to each measurement, the cuvette was irradiated with light from a 385 nm LED for 300 s and immediately loaded into the spectrometer. Due to the large molar absorptivity and high photoisomerization quantum yield of the azoheteroarene cations, the UV-Vis spectrometer probe light was sufficient to induce photoisomerization during the kinetics measurements. Consequently, it was necessary to operate the 385 nm probe light at low duty cycle to avoid perturbing the isomer populations.

Interaction between [2PA-MOEmim]$^+$ and methanol

As mentioned in the paper, the slower *Z-E* thermal isomerization rate of [2PA-MOEmim]$^+$ compared with [2PA-Bmim]$^+$ in methanol may be related to solvent hydrogen-bonding interactions with the ether substituent group. A systematic PM6 conformation search followed by ωB97X-D//cc-pVTZ geometric optimization identified the two structures shown in Figure S4 to be the *E* and *Z*-cluster global minima.[8] Calculated methanol bond dissociation energies are 49 kJ mol^{-1} and 54 kJ mol^{-1} for the *E* and *Z*-clusters, respectively.
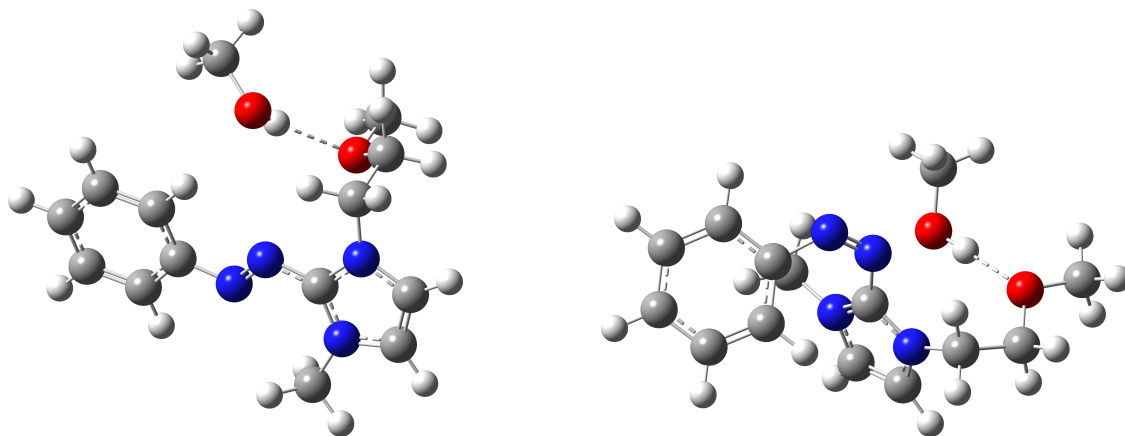
Figure S4: Calculated structures for [2PA-MOEmim]$^+$–methanol complexes with E (left) and Z (right) isomers.

References

(1) Chai, J.-D.; Head-Gordon, M. *Phys. Chem. Chem. Phys.* **2008**, *10*, 6615–6620.

(2) Dunning, Jr., T. H. *J. Chem. Phys.* **1989**, *90*, 1007–1023.

(3) Frisch, M. J. et al. Gaussian 09 Revision D.01. Gaussian Inc. Wallingford CT 2009.

(4) Campuzano, I.; Bush, M. F.; Robinson, C. V.; Beaumont, C.; Richardson, K.; Kim, H.; Kim, H. I. *Anal. Chem.* **2012**, *84*, 1026–1033.

(5) Besler, B. H.; K. M. Merz, Jr.,; Kollman, P. A. *J. Comp. Chem.* **1990**, *11*, 431–439.

(6) Revercomb, H. E.; Mason, E. A. *Anal. Chem.* **1975**, *47*, 970.

(7) May, J. C.; Goodwin, C. R.; Lareau, N. M.; Leaptrot, K. L.; Morris, C. B.; Kurulugama, R. T.; Mordehai, A.; Klein, C.; Barry, W.; Darland, E.; Overney, G.; Imatani, K.; Stafford, G. C.; Fjeldsted, J. C.; McLean, J. A. *Anal. Chem.* **2014**, *86*, 2107–2116.

(8) Stewart, J. J. P. *J. Mol. Model.* **2007**, *13*, 1173–1213.